AUTOMATED QUANTIFICATION OF MORPHODYNAMICS FOR HIGH-THROUGHPUT LIVE CELL TIME-LAPSE DATASETS

German Gonzalez[1], *Ludovico Fusco*[2], *Fethallah Benmansour*[3], *Olivier Pertz*[2], *Kevin Smith*[4]

[1] Magnetic Resonance Imaging Group, MIT [2] Institute of Biochemistry, University of Basel
[3] Computer Vision Lab, EPFL [4] Light Microscopy and Screening Center, ETHZ

ABSTRACT

We present a fully automatic method to track and quantify the morphodynamics of differentiating neurons in fluorescence time-lapse datasets. Our approach is capable of robustly detecting, tracking, and segmenting all the components of the neuron including the nucleus, soma, neurites, and filopodia. It is designed to be extremely efficient, capable of processing each image in approximately two seconds on a conventional notebook computer. To validate our approach, we analyzed neuronal differentiation videos in which a set of genes was perturbed using RNA interference. Our analysis quantifes and confirms morphodynamic behaviors which had been previously observed by biologists but never measured. Finally, we present new observations on the behavior of neurons made possible by our analysis which could not be discovered through static analyis.

Index Terms— Molecular and cellular screening; Image sequence processing; Fluorescence microscopy

1. INTRODUCTION AND RELATED WORK

The process of forming functional connections between neurons is complex and dynamic. Time-lapse microscopy has revealed that differentiating neurons undergo a large range of dynamic processes including cell body motility, filopodial dynamics, and repeated cycles of neurite growth and retraction. Of critical importance is the process by which axons and dendrites are formed in which a neurite ceases retracting, extends a long distance, and forms a connection. Such dynamic events are governed by a complex protein network that coordinates dynamic functions within the cytoskeleton, membrane, etc.

Powerful tools such as RNA interference (RNAi) technology, fluorescent protein labeling, image processing, and automated high-throughput microscopy have opened the door for large scale perturbation studies to help investigate such processes. RNAi screens have already led to novel insights into a number of cellular processes such as cell migration [1] and endocytosis [2]. However, limitations in image processing have restricted most investigations to static image analysis.

Knowledge of dynamics is essential if we are to understand complex processes such as neuron morphogenesis. However, designing algorithms to quantify dynamic behaviors is challenging, and automatic methods have appeared only very recently. State-of-the-art high-throughput techniques have successfully quantified morphodynamics of HeLA cancer cells in an effort to understand the process of mitosis [3, 4, 5]. However, the morphology and dynamics of these cell types are relatively simple compared to neurons, whose highly deformable neurites branch, expand, retract, and collapse.

In this paper, we propose a fully automatic method for detecting, tracking, and segmenting *every component of the neuron* (nucleus, soma, neurites, and filopodia), and quantifying their dynamic behaviors in ways that were previously not possible. Our approach first detects nuclei at each time step. A greedy tracking algorithm associates detected nuclei belonging belonging to the same neuron, forming a list of detections corresponding to that neuron. Using the detected nuclei as seed points, a region-growing algorithm segments the neuron's soma. The somata are used to initialize a joint segmentation of the entire structure of all neurons appearing in a image using a probabilistic method based on shortest path computations. A graph describing the morphology of the neurites is extracted from this segmentation. Each neurite tree is tracked by association, and filopodia are detected by analyzing the topology of the tracked neurites. Finally, a set of 156 *morphodynamic features* is extracted, quantifying the behavior of the each neuron in the video.

As demonstrated in Fig. 1, our approach produces reliable segmentations capable of capturing complex neuron dynamics. To validate our approach, we analyzed a small-scale siRNA screen of 5 genes (3 siRNAs/gene). Our analysis confirmed steady-state phenotypes obtained previously using MetaMorph™ [6]. We were also able to quantify dynamic behaviors which had been previously observed, but never measured [6]. Our analysis also uncovered new dynamic behaviors which are only apparant through dynamic analysis.

2. HIGH-THROUGHPUT TRACKING AND SEGMENTATION

The input to our approach is a series of T images $\mathcal{I} = \{I_1, \ldots, I_t, \ldots, I_T\}$ from which we extract K nucleus detec-

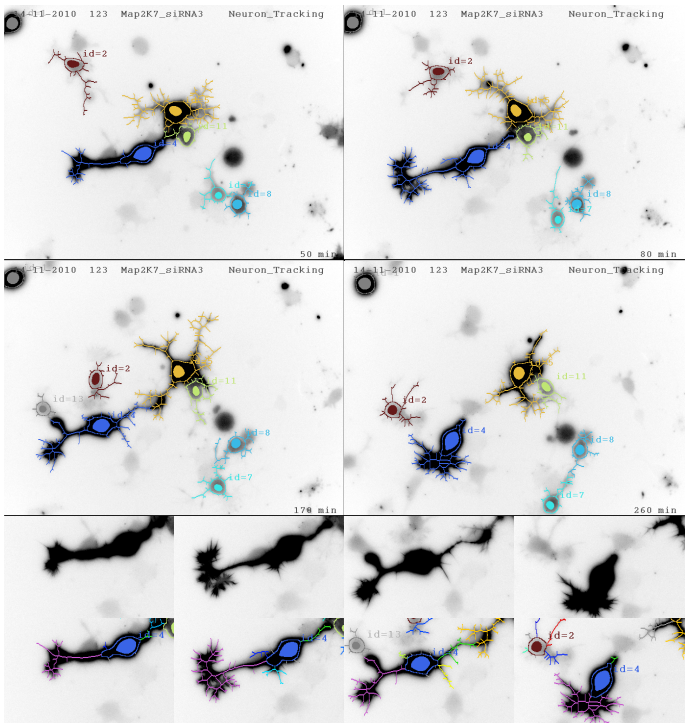

Fig. 1: *Neuron Tracking Results.* The top two rows contain frames from an experiment where MAP2K7 gene functions are inhibited. For visibility we enhanced the image contrast. Tracked neurons are marked by a unique color and id tag. Nuclei are denoted by filled ellipsoids, somata as contours, and neurites as trees. Bottom rows show details from above: 1) enhanced original image 2) tracked neurites marked with a different colors. Our approach performs well even in challenging situations where neurons appear in close proximity. Note: faintly stained cells are ignored for robustness.

tions d_t^k. The tracking step described in Sec. 2.2 associates valid detections across time steps while rejecting spurious detections. Since each neuron contains only one nucleus, there is a one-to-one mapping between each valid nucleus detection c_t^i and a neuron X_t^i. Thus, the tracking task is to provide a set of neuron detections $\mathcal{X}^i = \{X_a^1, \ldots, X_t^i, \ldots, X_b^i\}$ defining an individual neuron i from time $t = a$ to $t = b$. As depicted in Fig. 2, each neuron detection X_t^i is composed of a nucleus c_t^i, a soma s_t^i, a set of J neurites $\{n_t^{i,1}, \ldots, n_t^{i,j}, \ldots, n_t^{i,J}\}$, and a set of L filopodia associated with each neurite $F_t^{i,j} = \{f_t^{i,j,1}, \ldots, f_t^{i,j,l}, \ldots, f_t^{i,j,L}\}$ so that $N_t^i = \{(n_t^{i,1}, F_t^{i,1}), \ldots, (n_t^{i,j}, F_t^{i,j})\}$. Thus, a complete neuron i is described by $X_t^i = \{c_t^i, s_t^i, N_t^i\}$ at time step t.

2.1. Nuclei and Somata Detection and Segmentation

The first step in our approach is to extract a set of nucleus detections $\{d^1, \ldots, d^K\}$ over the image series. We worked with two-channel images where the cytoskeleton is marked with Lifeact-GFP and nuclei are marked with NLS-mCherry. The nuclie can be reliably detected and segmented by simply thresholding the NLS-mCherry channel and performing a morphological filling operation. Alternatively, one could apply a fast machine learning detector such as the one in [7].

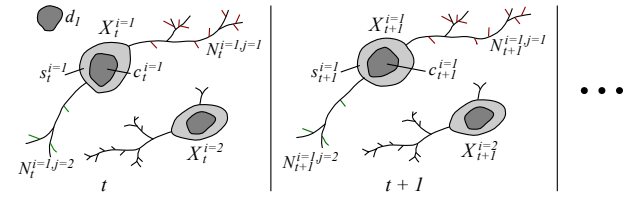

Fig. 2: *Neuron Tracking Notation.* A neuron i is defined by a time-series of neuron detections $\mathcal{X}^i = \{X_a^1, \ldots, X_t^i, \ldots, X_b^i\}$. The tracking returns a set $\mathcal{X}^i$ for each neuron i. At time t a neuron detection $X_t^i = \{c_t^i, s_t^i, N_t^i\}$ contains a nucleus c_t^i, a soma s_t^i, and a set of neurite-filopodia tuples $N_t^i = \{(n_t^{i,1}, F_t^{i,1}), \ldots, (n_t^{i,j}, F_t^{i,j}), \ldots, (n_t^{i,J}, F_t^{i,J})\}$ which contains J neurites and their associated filopodia shown in red for $j = 1$ and green for $j = 2$. A spurious nucleus detection d_1 is also shown.

Using the nuclei as seed points, somata are segmented as follows. A list of pixels neighboring the current soma segmentation is maintained. At each iteration, the neighbor with the smallest weighted distance to the centroid of the seed nucleus detection $D = \lambda||u - d^k|| + |I(u) - \hat{I}(d^k)|$ is added to the soma so long as $D < Y$, where u is a location in the image, $I(u)$ is the pixel intensity at that location, $\hat{I}(d^k)$ is the mean intensity of detection d^k, and Y is a threshold.

2.2. Efficient Tracking of Nucleus Detections

The tracking algorithm searches through the full set of nuclei detections and iteratively associates the most similar pairs of detections, returning lists of valid detections corresponding to each neuron $\mathcal{X}^i$. This is accomplished by constructing a graph $\mathcal{G} = (\mathcal{D}, \mathcal{E})$ where each node $d_t^k \in \mathcal{D}$ corresponds to a detection. For each detection d_t^k in time step t, edges $e \in \mathcal{E}$ are formed between d_t^k and all past and future detections within a time window W. A weight w_e is assigned to each edge according to spatial and temporal distances, and a shape measure $w_e = \alpha||d_{t1}^k - d_{t2}^l|| + \beta|t1 - t2| + \gamma f(\nu_{t1}^k, \nu_{t2}^l)$ where $e^{k,l}$ connects d_t^k and d_t^l, and ν^k is a shape feature vector containing d_t^k's area, perimeter, mean intensity, and major and minor axis lengths of a fitted ellipse. f evaluates differences between a feature a extracted from d_t^k and d_t^l as $f(a^k, a^l) = \frac{|a^k - a^l|}{|a^k + a^l|}$. The tracking solution corresponds to a set of edges $\mathcal{E}' \subset \mathcal{E}$ that minimizes the cost $\sum_{e \in \mathcal{E}'} w_e$.

To minimize this cost function, we adopt a greedy selection algorithm outlined in Table 1 and summarized in Fig. 3 that iteratively selects an edge with minimum cost $\hat{w}_e$ and adds it to the set $\mathcal{E}'$, removing future and past connections from the detections $e^{k,l}$ connects. The algorithm iterates until the minimum cost $\hat{w}_e$ is greater than a threshold Q. The track for neuron i is extracted from $\mathcal{E}'$ by traversing the graph $(\mathcal{G}, \mathcal{E}')$ and appending linked nucleus detections to $\mathcal{X}^i$.

2.3. Probabilistic Neuron Segmentation and Neurite Tree Extraction

Given an image I_t and the set of somata present in it $S_t = \{s_t^1 \ldots s_t^m\}$, our goal is to associate to each pixel u a label

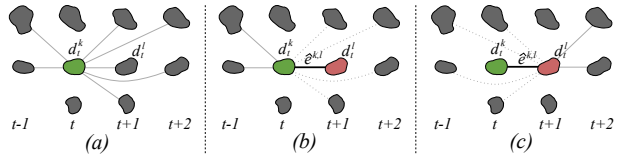

Fig. 3: *Efficient Tracking.* *(a)* The algorithm begins with each detection fully connected to all future and past detections within a time window W. Above, only d_t^k's edges are shown. *(b)* Each iteration, the edge $\hat{e}^{k,l}$ with minimum cost $\hat{w}_e$ is added to $\mathcal{E}'$. Edges connecting d_t^k to future detections are removed from $\mathcal{E}$. *(c)* Edges connecting d_t^l to the past are removed from $\mathcal{E}$. The process is repeated until $\hat{w}_e > T$.

$J_t(u)$ that indicates to which neuron (soma) it belongs. The probability of $J_t(u)$ can be deduced using Bayes' rule,

$$P(J_t(u) = i|S_t, I_t) = \frac{P(S_t, I_t|J_t(u) = i)}{\sum_{\eta=1}^{m} P(S_t, I_t|J_t(u) = \eta)}, \quad (1)$$

where we assume a uniform distribution on $P(J_t(u))$. The numerator is modeled as the probability of the path L that connects maximally the voxel u to the soma s_t^i, $P(S_t, I_t|J_t(u) = i) = \max_{L:u\to s_t^i} \prod_{\{l_r\}\in L} P(I_t(r)|l_r)$, where l_r are indicator variables for the locations forming the path L. We chose this model since an optimal maxima can be found by minimizing its negative likelihood using Dijkstra's shortest path and because it produces connected components.

To optimize this function, we map the image I_t to a graph $\mathcal{G}_t^i = (V, E)$ whose vertices u are the pixels in I_t and whose directed edges $e_{r,v}$ connect each pixel to its four neighbors. We assign to each edge a weight $w_{r,v} = -logP(I_t(v)|v)$. $P(I_t(v)|v)$ represents the probability that a neurite traverses a node v. It is obtained by applying a sigmoid function to the output of the tubularity filter of [8]. The parameters of the sigmoid function are estimated using maximum likelihood. Finally, we define the set of neurite pixels U_n^t as those that connect to any soma with a higher probability than ϵ. We predict their labels as the ones that maximize Eq. 1. The set of pixels associated to neuron X_t^i is the union of the neurites and the soma associated with i, $U_i^t = \{u \in U_n^t | J_t(u) = i\} \cup s_t^i$.

Algorithm 1 Tracking association algorithm

Start with an empty set $\mathcal{E}'$.
repeat
  Find edge $\hat{e}^{k,l}$ with minimum cost $\hat{w}_e$.
  Add $\hat{e}^{k,l}$ to $\mathcal{E}'$, linking detections d_{t1}^k and d_{t2}^l.
  Remove $\hat{e}^{k,l}$ from $\mathcal{E}$.
  if $t1 < t2$ **then**
    Remove edges between d_{t1}^k and *future* detections (where $t > t1$) from $\mathcal{E}$
    Remove edges between d_{t2}^l and *past* detections (where $t < t2$) from $\mathcal{E}$
  else
    Remove edges between d_{t1}^k and *past* detections (where $t < t1$) from $\mathcal{E}$
    Remove edges between d_{t2}^l and *future* detections (where $t > t2$) from $\mathcal{E}$
  end if
until $\hat{w}_e > T$

To reduce the neurite segmentation to a tree, we skeletonize the neuron and define as root node the pixel of the skeleton closest to the centroid of the nucleus. We instantiate a Minimum Spanning Tree from the root and create a neurite tree wherever the spanning tree exits the soma.

2.4. Neurite Tracking and Filopodia Detection

Neurites are tracked by applying the algorithm described in Sec 2.2 using the centroids of the neurite trees instead of nucleus centroids, with the additional constraint that edges may only exist between neurites that emanate from the same soma. Filopodia are detected by starting at each leaf node in a neurite and traversing the tree until a branch point is reached. If the distance traversed is less than a threshold T_f, the traversed locations are considered to be filopodia.

3. EXTRACTING MORPHODYNAMIC FEATURES

Our tracking and segmentation method produces sets of graphs linking detections, contours, and trees to define each neuron over time. This data structure is not immediately useful for quantifying dynamic behaviors. To facilitate the analysis, we extract a set of *156 meaningful features* from our data structure to quantify morphodynamics, which are too numerous to list here. A few examples for the nucleus and soma include: area, perimeter, Lifeact-GFP intensity, NLS-mCherry intensity, speed, acceleration, total distance traveled, time spent expanding/contracting, frequency of expansion. For neurites: number of branches, distance from tip to soma, filopodia length, number of filopodia, major axis, minor axis and eccentricity of an ellipse fitted to the neurite, total length, time spent expanding/contracting, frequency of expansion. We also compute change-over-time for each of the features mentioned above (denoted by Δ).

4. RESULTS

4.1. Experimental Setup

We applied our approach to data from a small-scale siRNA screen in which the functions of 5 genes were inhibited: SrGAP2, MAP2K7, RhoA, Trio, and Net. Three siRNAs were applied for each gene, producing a total of 17 experiments including 2 controls. 30 videos per experiment were obtained over the course of 3 days, with images taken at 20× magnification in 10 minute intervals. A total of 510 videos were collected, each containing approximately 100 2-channel images of 696 × 520 resolution. We tracked and segmented a total of 7,298 neurons (33,213 neurites), extracting morphodynamic features for each. Each video was processed in under 210 seconds on a Lenovo W510 notebook computer. The entire screen was processed in parallel in just a few hours using conventional PCs.

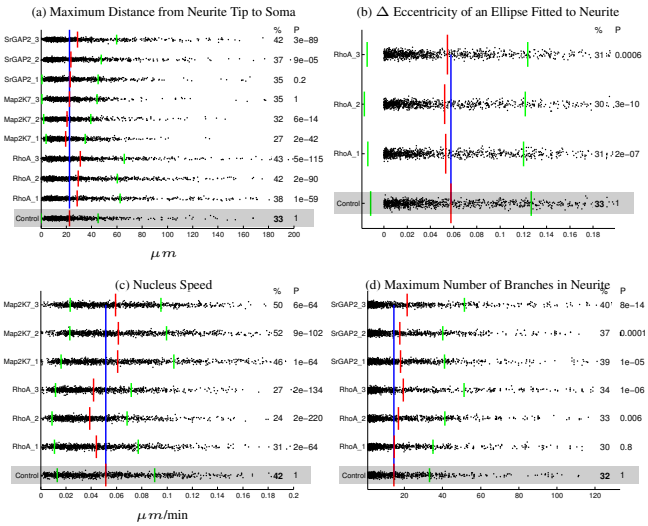

Fig. 4: *Quantitative Morphodynamic Analysis.* Four informative morphodynamic features are plotted, where the control experiment is marked in gray below the siRNA targets. Black dots represent collected data points. Red bars indicate the mean, green bars indicate standard deviation. The blue line shows the control's mean for comparison. Values under the % column are the percentage of data points above the control's mean. Values under P indicate the student-t test p-value. See text for details.

4.2. Analysis

Our goals were to 1) validate our approach by reproducing the findings of [6], 2) quantify previously observed but unmeasured morphodynamics, and 3) uncover new dynamic behaviors. A brief summary of our findings is provided below and in Fig 4. Further details can be found in our online supplementary tables and videos. All findings reported below have statistically significant measures, with a p-value $<< 0.05$.

Our analysis confirmed several effects previously observed through static image analysis in [6]. In particular, RhoA loss of function resulted in fewer but longer neurites than the control. SrGap loss was found to have longer neurites, and Map2K7 loss was found to have more neurites but of shorter length. These findings were confirmed by static measures from our experiments: the mean longest neurite length – control 22.6μm, RhoA-3 32μm, SrGap2-1 28.9μm, and Map2K7-1 19.5μm (see Fig. 4a)[1]; and by a dynamic measure – the mean number of neurites belonging a neuron over its lifetime: control 3.4, RhoA 3.1, and Map2K7-1 3.9.

It had been previously observed, but never quantified, that loss of SrGap2 function produces a high number of filopodia, and that RhoA loss results in neurites that easily extend but have difficulty retracting. Morphodynamic features from our analysis confirmed these observations. Mean number of filopodia detected per neurite over its lifetime was 6.69 in the control and 8.81 for SrGap-3[1]. The mean change in elongation as measured by an ellipse fitted to the neurite was 5.7% for the control and 5.3% for RhoA-1 (see Fig. 4b)[1]. While this difference may seem small, it is statiscially significant due to the large amount of data collected (p-value is 2×10^{-7}).

Our quantitative analysis revealed new morphodynamics which were not obvious to human observers. We found that RhoA function loss slowed neuron motility and Map2K7 increased it. Control cells moved at .30 $\mu m/min$, RhoA moved at .23 $\mu m/min$, and Map2K7-2 moved at .37 $\mu m/min$ (see Fig. 4c). We also found that RhoA and SrGap increased the branching of the neurites (see Fig. 4d). Over the course of a neurites lifetime, the maximum number of branches in a control neuron was 14.5, 19.44 for RhoA-3, and 21.39 for SrGap2-3[1].

5. CONCLUSION

We have described a a fully automatic method to track and quantify the morphodynamics of differentiating neurons in fluorescence time-lapse datasets. Our approach is capable of robustly detecting, tracking, and segmenting all the components of the neuron including the nucleus, soma, neurites, and filopodia. Our approach is extremely efficient, and is capable of quantifying morphodynamics of neurons through 156 meaningful features. Using our approach, we were able to reproduce previous findings from a static analysis, quantify behaviors that had been previously observed but never measured, and uncover dynamic phenotypes. In the future, we plan to expand this work to a larger scale screen and develop statistical techniques to infer relationships between genes and morphodynamic phenotypes.

6. REFERENCES

[1] Bakal, C., et al.: Quantitative Morphological Signatures Define Local Signaling Networks Regulating Cell Morphology. Science **316** (2007) 1753–1756

[2] Collinet, C., et al.: Systems Survey of Endocytosis by Multiparametric Image Analysis. Nature **464** (2010) 243–249

[3] Held, M., et al.: CellCognition: time-resolved phenotype annotation in high-throughput live cell imaging. Nature Methods **9**(7) (2010) 747–754

[4] Neumann, B., et al: Phenotypic profiling of the human genome by time-lapse microscopy reveals cell division genes. Nature **464** (2010) 721–727

[5] Zhu, C., et. al: Functional analysis of human microtubule-based motor proteins, the kinesins and dyneins, in mitosis/cytokinesis using RNA interference. Cell **16** (2005) 3187–3199

[6] Pertz, O., et al: Spatial Mapping of the Neurite and Soma Proteomes Reveals a Functional Cdc42/Rac Regulatory Network. Proc. Natl. Acad. Sci. **105** (2008) 1931–1936

[7] Smith, K., Carleton, A., Lepetit, V.: Fast Ray Features for Learning Irregular Shapes. In: ICCV. (2009)

[8] Frangi, A.F., Niessen, W.J., Vincken, K.L., Viergever, M.A.: Multiscale Vessel Enhancement Filtering. Lecture Notes in Computer Science **1496** (1998) 130–137

[1] Only neurons containing the 10^{th} percentile of longest neurites were considered.